

This article was downloaded by:[Bochkarev, N.]  
On: 12 December 2007  
Access Details: [subscription number 746126554]  
Publisher: Taylor & Francis  
Informa Ltd Registered in England and Wales Registered Number: 1072954  
Registered office: Mortimer House, 37-41 Mortimer Street, London W1T 3JH, UK



## Astronomical & Astrophysical Transactions

### The Journal of the Eurasian Astronomical Society

Publication details, including instructions for authors and subscription information:  
<http://www.informaworld.com/smpp/title~content=t713453505>

#### The spatial anisotropy of flares with respect to sunspot groups and vector butterfly diagrams in solar activity cycles 17-20

V. V. Kasinsky <sup>a</sup>

<sup>a</sup> Irkutsk Institute of Transport Engineers, Irkutsk, Russia

Online Publication Date: 01 January 1999

To cite this Article: Kasinsky, V. V. (1999) 'The spatial anisotropy of flares with respect to sunspot groups and vector butterfly diagrams in solar activity cycles 17-20', *Astronomical & Astrophysical Transactions*, 17:5, 341 - 350

To link to this article: DOI: 10.1080/10556799908244083

URL: <http://dx.doi.org/10.1080/10556799908244083>

PLEASE SCROLL DOWN FOR ARTICLE

Full terms and conditions of use: <http://www.informaworld.com/terms-and-conditions-of-access.pdf>

This article maybe used for research, teaching and private study purposes. Any substantial or systematic reproduction, re-distribution, re-selling, loan or sub-licensing, systematic supply or distribution in any form to anyone is expressly forbidden.

The publisher does not give any warranty express or implied or make any representation that the contents will be complete or accurate or up to date. The accuracy of any instructions, formulae and drug doses should be independently verified with primary sources. The publisher shall not be liable for any loss, actions, claims, proceedings, demand or costs or damages whatsoever or howsoever caused arising directly or indirectly in connection with or arising out of the use of this material.

# THE SPATIAL ANISOTROPY OF FLARES WITH RESPECT TO SUNSPOT GROUPS AND VECTOR BUTTERFLY DIAGRAMS IN SOLAR ACTIVITY CYCLES 17–20

V. V. KASINSKY

*Irkutsk Institute of Transport Engineers, 664074, Irkutsk, Russia*

*(Received March 1, 1998)*

Data on the location of flares covering solar cycles 17–20 were used to construct vector  $R(\varphi, t)$  diagrams for the mean position of the flare scattering centre in the coordinate system of the sunspot centre. The  $R(\varphi, t)$ -diagram reveals a spatial anisotropy of the flare process relative to the midline of the  $\varphi - t$ -diagram. The  $R_\varphi$ -component is always directed towards the central midline of the diagram. In turn, the  $R_\lambda$ -component has a character of oppositely directed shears relative to the central midline of the diagram. Thus high-latitude sunspots exhibit a positive  $R_\lambda > 0$  (westward) displacement, while low-latitude sunspots show a negative  $R_\lambda < 0$  (eastward) one. The vector diagrams of flares reveal a global anisotropy of the flare process. The results are interpreted in terms of a global-scale excitation of flares by wave-like disturbances.

KEY WORDS Flares, butterfly diagrams, spatial anisotropy

## 1 INTRODUCTION

The Maunder diagrams of the sunspots known as the “butterfly diagrams” (BD) have existed since 1901 and serve as a good illustration of the Sporer law (Gibson, 1973). Investigation of the latitude-time distribution of sunspot areas for cycles 17 to 20 indicates the presence of sunspot formation “impulses” for different latitude-time intervals on the BD (Antalova and Gnevyshev, 1983). Similarly, latitude-time BD of flares in activity cycles 18 and 19 show the presence of distinct “fine structure” in the number of flares (Krivsky and Knoshka, 1967). Fine structure of the  $\varphi - t$ -diagrams raises a more general question as to whether the distribution of flares in the coordinate system of related sunspots is isotropic and independent of the position of sunspots on the BD. Indeed, sunspot groups at the centre of the  $\varphi - t$ -diagram are closely packed together and interact with each other intensively, whereas at the periphery of the diagram this interaction decreases with the distance from the centre of the diagram.

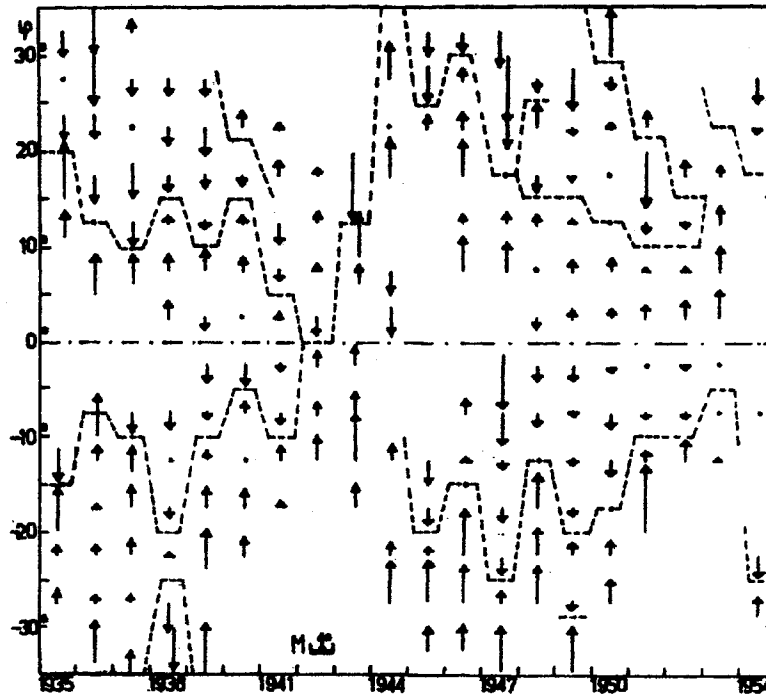


Figure 1 The vector diagram of the  $R_{\varphi}$ -component of flare displacement in the coordinate system of the sunspot centre. The vectors represents the mean calculated for period (1935–1954) within the latitude-time interval  $5^{\circ} \times 0.5$  year.

This problem cannot be solved by studying only scalar BD. It is necessary to study the mutual arrangement of sunspot and flares, i.e. to construct a vector diagram. The simplest way of obtaining it is to investigate mean displacements of flares relative to sunspots as a frame of reference in which the events take place. The objective of this paper is to construct vector butterfly diagrams (VBD) for a mean position of flares  $R(\varphi, t)$  for a period of several solar cycles (1934–1976). The second aim is to give a general interpretation of the vector diagrams in the terms of existing models of solar flares.

## 2 METHOD. LATITUDINAL VECTOR BUTTERFLY DIAGRAMS OF FLARES IN SOLAR CYCLES 17–20

In the previous papers it was found that the N–S asymmetry of the flare locations relative to the sunspot centre varied regularly with latitude  $\varphi$  and phase ( $t$ ) of the cycle (Kasinsky, 1973, 1981). Data are taken from the “Quarterly Bulletin on Solar Activity” (1935–1976) as the base catalogue, tables “éruptions chromosphériques” and “régions actives” of the bulletin. Coordinates  $(\varphi, \lambda)$  of over 10 000 flares were

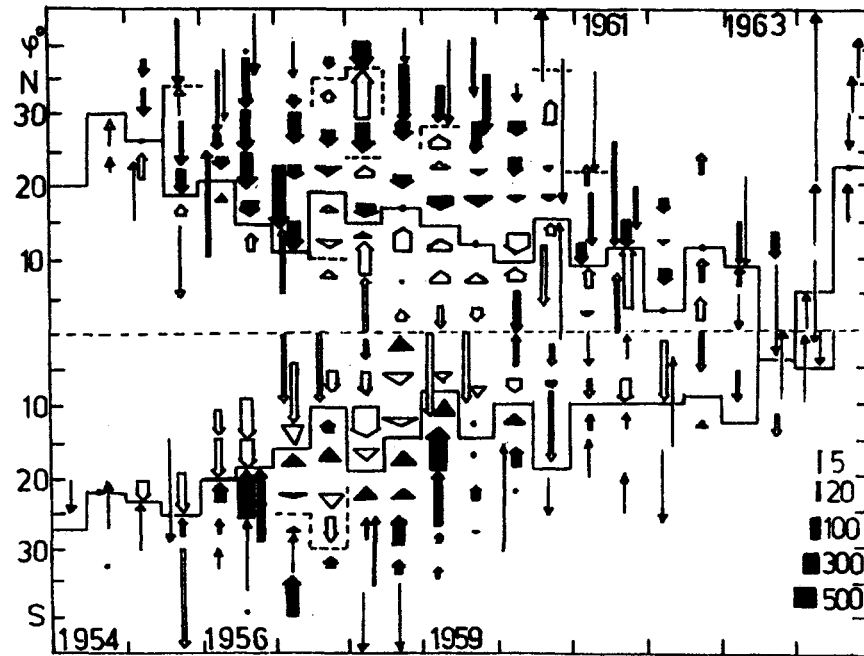


Figure 2 The vector diagram of the  $R_\varphi$ -component of flare constructed with allowance made for "weight" of  $R$  (number of flares) in the 19-th cycle. The "weight" is shown by the width of the arrows. The scale of  $R$  is  $5 \times 1^\circ$  of the scale of latitude axis.

used in the analysis. The mean position of the flare scattering centre with respect to the sunspot group was calculated by the formula:

$$\langle R_\varphi \rangle = \frac{1}{N} \sum_i \sum_s (\varphi_{is} - \varphi_s), \quad (1)$$

where  $\varphi_{is}$  is the flare's latitude in the  $s$ -sunspot,  $\varphi_s$  is the latitude of the sunspot's centre, and  $N$  is a total number of flares. The summation in (1) is made twice; first, over all flares ( $i$ ) in a given sunspot ( $s$ ) and, then, over all groups ( $s$ ) falling within the latitude-time interval  $\Delta\varphi\Delta t = 5^\circ \times 0.5$  year in this case. Figure 1 presents the  $\varphi - t$ -diagram of the  $R_\varphi$  component of flare displacement calculated for each year of the time interval 1935–1954. The period including cycles 17, 18.

The results showed quite clearly that the absolute value of vector  $|R_\varphi|$  increased as the diagram periphery approached, while the flare vectors consistently pointed to the diagram centre at which the flare scattering tended to be isotropic,  $R_\varphi \rightarrow 0$ .

Figure 1 means that the flare process is anisotropic with respect to the centre of the  $\varphi - t$ -diagram in such a way that their mean positions are systematically displaced to the centre of the diagram. Hence, the spatial characteristics of flare generation in sunspots strongly depend on their position on the diagram. The distribution of flares becomes homogeneous and isotropic only on the midline of the

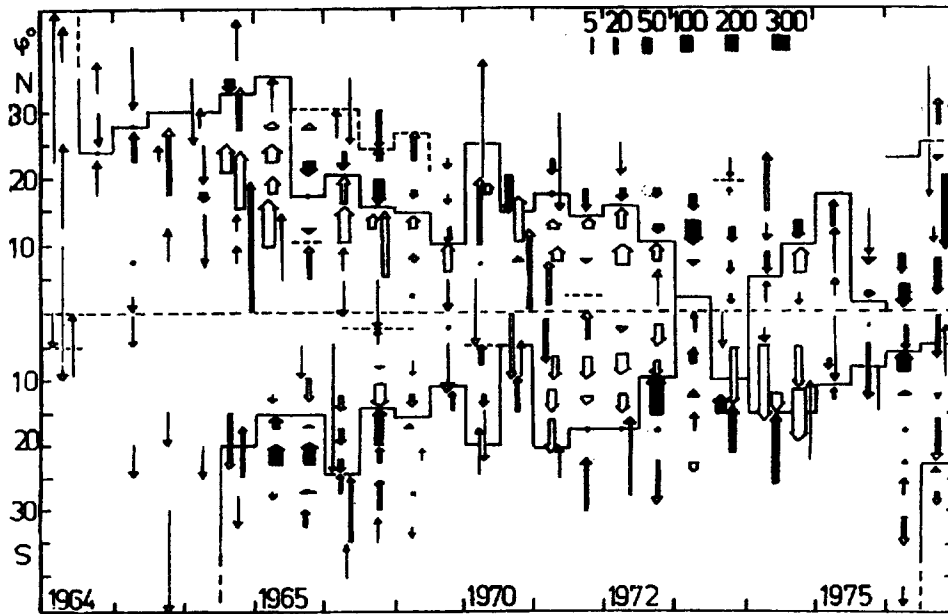


Figure 3 The vector diagram of the  $R_\varphi$ -component of flare constructed with allowance made for "weight" in the 20-th cycle. The "midline" of isotropization of flares is shown by the step-like line. The designations and scale as in Figure 2.

diagram. This midline can be identified as the zero displacement line  $\langle R_\varphi \rangle = 0$ . The areas in which the flare distribution becomes isotropic is traced by the dashed lines in Figure 1. One can see that midlines start at high latitudes ( $30^\circ$ ) and are descending towards the equator, following Sporer's law.

The VBD of flares constructed with allowance made for "weight" are shown in Figures 2 and 3. The "weight" of vectors is the number of flares in the relevant area of the  $\varphi - t$ -diagram and is shown by the width of the arrows. The scale of the vectors in Figures 2 and 3 is magnified 5 times as compared with the scale of the latitude axis. The areas of isotropic distribution of flares are determined by the  $|R_\varphi| = 0$  condition (the step-like line). The main shifts are depicted differently; the light arrows give a polar type, and the dark arrows give an equatorial type of shifts (Kasinsky, 1988, 1989). The line of isotropization of flares divides each wing of the "butterfly" into two asymmetric halves with the opposite direction of  $R_\varphi$ .

Assessing the significance of the mean displacements of flares obtained involved calculating the r.m.s deviation of  $\langle R_\varphi \rangle$ . The error of the mean  $R_\varphi$  is  $\sigma_n = s/\sqrt{n}$  where  $n$  is the number of flares in a sunspot. At a given r.m.s. error in one measurement  $\sigma_0 \sim 1-2^\circ$ ,  $\sigma_n$  should decrease. Thus, when a  $5^\circ \times 1$  year average is taken,  $n \geq 100$ , the error in the mean displacement  $R_\varphi$  does not exceed  $+0.1-0.2^\circ$ . That is the  $R_\varphi$  is significant on 0.997 confidence level. A qualitative run of the

**Table 1.** The run of  $\pm\langle R_\varphi \rangle$ , r.m.s error and number of flares  $N$  (see the text)

Total flares $\pm\varphi$	10 525 Cycles 17+18			27 530 Cycle 19			38 055 Cycles 17+18+19		
	$\langle R_\varphi \rangle$	r.m.s	$N$	$\langle R_\varphi \rangle$	r.m.s	$N$	$\langle R_\varphi \rangle$	r.m.s	$N$
+30°				-0.01	±0.18	117	-0.01	±0.18	117
25°				-0.74	±0.09	543	-0.74	+0.09	543
20°	-0.76	±0.11	205	-0.12	±0.04	1283	-0.21	+0.05	1488
15°	-0.74	±0.05	801	-0.36	±0.03	2669	-0.45	+0.03	3470
10°	-0.54	±0.03	2015	-0.28	±0.02	4139	-0.36	+0.02	6154
+5°	-0.24	±0.02	3556	-0.35	±0.02	7580	-0.31	+0.02	11146
-5°	+0.25	±0.03	2536	+0.39	±0.03	5577	+0.34	+0.02	8113
-10°	+0.51	±0.11	1211	+0.15	±0.06	1034	+0.20	+0.03	5792
-15°	+0.50	±0.11	191	+0.15	±0.06	1034	+0.20	+0.04	1225
-20°				+4.60	+0.80	7	+4.60	±0.8	7

value of  $R_\varphi$ , the sign of  $R_\varphi$  the r.m.s error and the accumulated number of flares  $N$  are shown in Table 1 as a function of latitude zones for the cycles 17, 18 and 19. In Table 1 the “+” and “-” signs denote the polar and equatorial directions of  $R_\varphi$  respectively relative to the midline ( $R_\varphi = 0$ ) in Figures 1-3.

### 3 LONGITUDINAL VECTOR DIAGRAM OF FLARES

The longitudinal component of a mean displacement of flares was calculated using the data on longitude position of flares from the central meridian -  $\lambda$  (CM) according to the “Quarterly Bulletin on Solar Activity” (1935-1954). To reduce  $\lambda$  to the frame of reference tied to a sunspot group rotating on the solar surface, we used the formula of mean differential rotation (Alien, 1955). The flare position with respect to the sunspot’s centre is defined by:

$$\begin{aligned}\Delta\lambda_{is} &= \lambda_{is} - \omega(\varphi)[(t_{is} - t_s(\text{cmp})], \\ \omega(\varphi) &= 13^\circ 38' - 2^\circ 77' \sin^2 \varphi,\end{aligned}\quad (2)$$

where  $\lambda_{is}$  is central meridian distance of the  $i$ s-th flare,  $t_{is}$  is the flare onset time, and  $t_s$  is the time of sunspot group passage through the central meridian (cmp),  $\omega(\varphi)$  is the diurnal angular velocity of synodic rotation of sunspots at the latitude  $\varphi_s$ . As done in formula (1), we take a double average, first over all flares in a given sunspot and, secondly, over all sunspots in a given interval of  $\varphi - t$ -diagram:

$$\langle R_\lambda \rangle = \frac{1}{N} \sum_i \sum_s (\Delta\lambda_{is}). \quad (3)$$

The vector diagram  $R_\lambda$ -component of flares thus calculated is shown in Figure 4. For the sake of illustration, the scale of vectors  $R_\lambda$  is taken to be ten times larger as compared with that of the latitude axis. The value of  $R_\lambda$  varies in the range

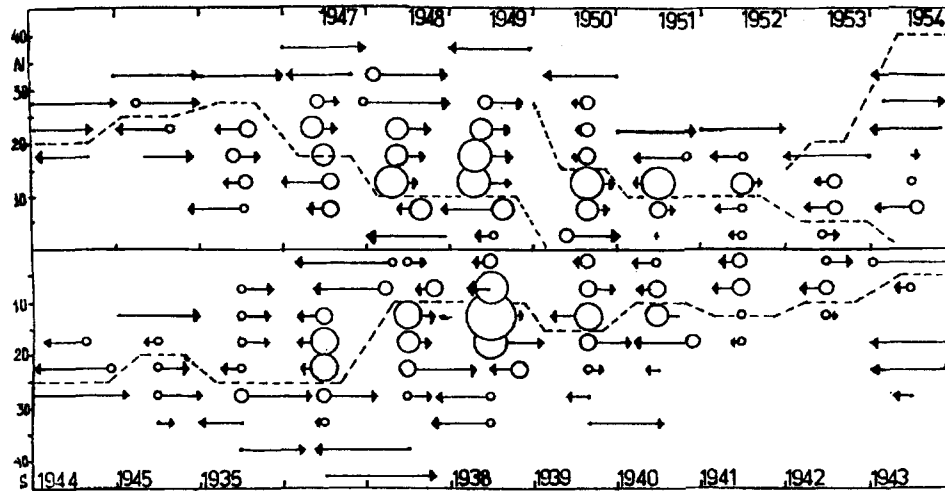


Figure 4 Vector diagrams for longitudinal displacement of the flare in the 17-th and 18-th cycle superimposed. The step-like broken lines represents zero line of  $R_\lambda = 0$ . The scale of  $R$  is  $5 \times 1^\circ$  of the scale of latitude axis.

from  $0.5^\circ$  to several degrees. As in the case of vector diagrams for latitudinal displacements (Figure 1), it is possible to draw zero lines  $R_\lambda = 0$  which divide the  $\varphi - t$ -diagram into areas with the opposite character of the direction of  $R_\lambda$ . As these lines cross in the  $\varphi$ -direction, the sign of  $R_\lambda$  changes for the opposite. As is evident from Figure 4, the ( $R_\lambda = 0$ )-lines are drifting from high to low latitudes, according to Sporer's law on the whole.

Specifically, below the  $\varphi - t$ -diagram midline the displacements are directed eastward ( $R_\lambda < 0$ ), and above the midline they are directed westward ( $R_\lambda > 0$ ). We shall call this type of  $\pm R_\lambda(\varphi, t)$  asymmetry a "normal" type. The opposite type of asymmetry occurs more rarely. The normal  $R_\lambda$  asymmetry shows also a tendency for the absolute value of  $|R_\lambda|$  to increase with increasing distance from the  $\varphi - t$ -diagram centre.

In order to identify more clearly the regular tendency of  $R_\lambda$ -asymmetry, it is possible to average the  $R_\lambda(\varphi, t)$  pattern depicted in Figure 4 over the two cycles (17+18) and two hemispheres ( $N + S$ ) of the diagram. To obtain the correct averaging, the two cycles were superimposed by their maximum epoch with the time step of 1 year. Then the superposition of  $N, S$ -hemispheres were taken.

The superposition of the  $R_\lambda(\varphi, t)$  pattern was made for  $0 + 25^\circ$  latitudes at steps of  $5^\circ$ . The result of such averaging is presented in Figure 5. Circles shown give the relative absolute number of flares which was used in averaging and totaled 8300 flares (76%) of the initial number of flares. The length of the  $t$ -axes equals that of an 11-year cycle. It is quite evident from Figure 5 that there is an oppositely directed  $\pm R_\lambda$  displacement which increases in absolute values as one moves away from the midline  $\varphi - t$ -diagram.

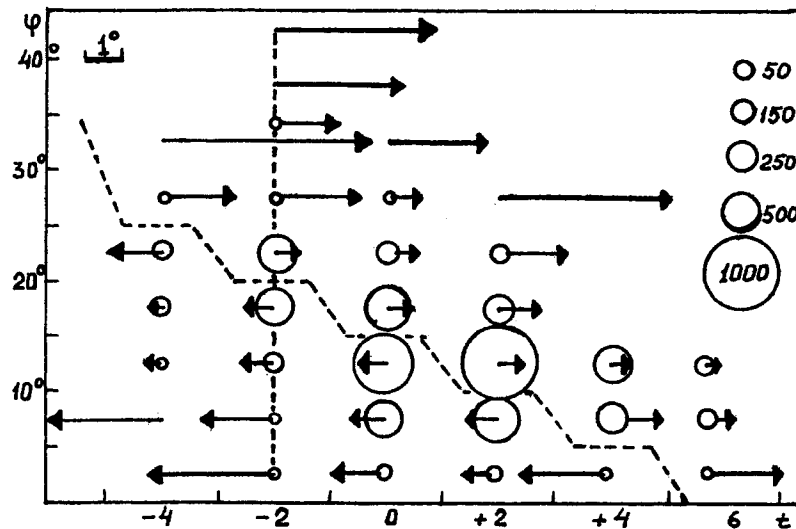


**Figure 5** Vector diagrams for longitudinal displacement of the flares in the 17-th and 18-th cycle averaged over the four wings of the diagram (Figure 4). The  $t$ -axis is in years from maxima epoch (zero). The scale of arrows is  $3 \times 1^\circ$  of the scale of latitude axis.

It is apparent from Figure 5 that the system of E-W like shifts on the  $\varphi - t$ -diagram has a tendency to persist during the course of an 11-year cycle as the zero midline descends to the solar equator. As in the case of Figure 4 the zero midline ( $R_\lambda = 0$ ) is drifting from high to low latitudes, according to Sporer's law on the whole. Therefore this midline is to be identified with the drifting sunspot formation "trajectory" on the  $\varphi - t$ -diagram.

The mean value of  $R_\varphi$  from (1) and corresponding value of  $R_\lambda$  from (4) form the components of vector  $\mathbf{R}(\varphi, t)$  which can be referred to each point on the  $\varphi - t$ -diagram. Therefore this vector butterfly diagram of flares characterizes the magnitude and direction of non-isotropization of the flare distribution in the sunspots on the  $\varphi - t$ -diagram as was initially proposed in (Kasinsky, 1973,1981). So far, as  $R_\varphi$ -component is always directed towards the central line of the  $\varphi - t$ -diagram, this centre must play some role in the process of flare's activity.

#### 4 LONGITUDINAL VECTOR DIAGRAM OF FLARES AS THE ABERRATION EFFECT

From the previous sections it necessarily follows that the centre of the vector diagram  $R(\varphi, t)$  is physically significant. Among other things it may serve as a possible source for a global, triggering disturbance with regard to flares. We also may assume that this triggering disturbance gives rise to a flare at a point within the group which is reached as a result of the propagation across the rotating Sun

from mid  $\varphi_0$  latitude of the diagram to a given  $\varphi_s$  sunspot's latitude. Because different sunspots belong to different zones of rotation, the high-latitude sunspots will lag behind the disturbance, while those near the equator, in which the groups rotate faster, will overtake the disturbance. In other words, the high-latitude zones will show a positive,  $R_\lambda > 0$ , westward shift of flares, while low-latitude zones will show a negative, westward one,  $R_\lambda < 0$ . Those opposite  $\pm R_\lambda(\varphi)$  shifts on the high and low latitudes may be interpreted as the longitudinal aberration effect of flares (Kasinsky, 1994).

It is well-known that the aberration of light gives for the angular displacement  $\beta$  of the visual position of a star:

$$\tan \beta = V/C, \quad (4)$$

where  $V$  the observer's velocity, and  $C$  the velocity of light, (Blazhko, 1954). Instead of  $V$  in (5), we should substitute the velocity difference of the sunspots due to differential rotation,  $V(\varphi_s) - V(\varphi_0)$ , where  $\varphi_s$  is the flaring sunspot latitude, and  $\varphi_0$  is the mean latitude on the  $\varphi - t$ -diagram which is supposed to be a primary source of the flare trigger.

Let us assume that some wave-like disturbance is generated at the latitude  $\varphi_0$  and propagates to the latitude  $\varphi_s$  with the velocity  $C$ . The initial angular velocity  $\omega_0$  is given by (3) and linear velocity  $V_0$  should be:

$$V_0 = R_\otimes \omega(\varphi_0) \cos \varphi_0 = R_\otimes (a - b \sin^2 \varphi_0) \cos \varphi_0,$$

where  $R_\otimes$  is the Sun radius. The sunspot located at the latitude  $\varphi_s$  will have a velocity due to its own rotation for a value:

$$V_s = R_\otimes (a - b \sin^2 \varphi_s) \cos \varphi_s.$$

Substituting instead of  $V$  the difference  $V_0 - V_s$  in (5) we shall have:

$$\tan \beta = R_\otimes [a(\cos \varphi_0 - \cos \varphi_s) - b(\sin^2 \varphi_0 \cos \varphi_0 - \sin^2 \varphi_s \cos \varphi_s)]/C. \quad (5)$$

Bearing in mind that  $\tan \beta \sim \beta = |R_\lambda|/(\varphi_s - \varphi_0)$ , from (6) it is apparent that the high-latitude sunspots,  $\varphi_s > \varphi_0$  will give a positive shift,  $\tan \beta > 0$ , while those in low-latitudes will give a negative one,  $\tan \beta < 0$ . Therefore, the determination of  $C$  reduces to finding the aberration angle  $\beta$ . According to Figure 5, the angle  $\beta \sim 8^\circ$ . Taking  $\beta = 8^\circ$  ( $\tan \beta = 0.16$ ) for  $\varphi_s = 0^\circ$  and  $\varphi_s = 20^\circ$  in (6), we obtain for the mean value of  $C \sim 1.1$  km/s. So we can take  $C = 1$  km/s as a good estimate for the flare trigger velocity. The type of disturbance may be the internal gravity waves in the compressible atmosphere (More, 1964) propagating with subsonic velocities 1–2 km/s in accordance with the velocity value obtained.

## 5 DISCUSSION

In spite of the appreciable progress made so far in the observation and modelling of solar flares there does not exist a full-blown theory of flares. The most well-developed theory is the magnetic annihilation in the current sheets of corona (Syrovatsky, 1966; Somov, 1981). Pogodin (1977) made an attempt to interpret the

early vector diagrams of flares (Kasinsky, 1973) in terms of the interaction of the background magnetic and the main active region fields. His interpretation is in general agreement with the available models of solar flares (Krivsky, 1977; Somov, 1981).

However, analysis of the energetics of large flares has shown that on the upper limit of energy ( $10^{32}$  erg) and masses ( $10^{16}$ – $10^{17}$  g) in the corona there exist no relevant “accumulators” of energy (Gershberg, Mogilevsky, Obridko, 1987). Moreover, in the magnetic models of flares the main problem remains a mystery as regards magnetic field annihilation. Therefore, the alternative sources of energy may exist, i.e. magnetohydrodynamic waves which transfer energy itself, so called “soliton” model proposed by Mogilevsky (1980).

The detection of a spatial anisotropy of the flares on the  $\varphi - t$ -diagram imposes certain limitations on models of the flare process. In particular the  $R_\varphi$  spatial anisotropy of flares distinguishes between the direction to the centre of VBD and its periphery. It is more likely that overall tendency for  $R_\varphi$ , shifts towards the centre of the VBD indicates that in the coordinate system of sunspots generating flares there exists some disturbance, originating from the diagram centre. Because sunspot drift in latitude is negligible, the  $R_\varphi$  shifts of flares cannot be accounted for by the centrifugal drift of sunspots out of the diagram centre. It is more likely that the  $R_\varphi(\varphi, t)$  pattern is explained in a more direct manner. Namely the midline of VBD gives rise to a certain constantly acting trigger-like disturbance which, when reaching the sunspots lying at the periphery of the diagram, causes the observed  $\pm R_\lambda$  displacements. Generally the agent of a disturbance may be associated with some type of magneto-hydrodynamic waves (Gibson, 1973). The type of disturbance might also be a long gravity wave like tsunami proposed by Kassinsky and Krat (1973). If the generation of flares in sunspots depended only on internal factors, this feature of the  $R(\varphi, t)$  would be hard to explain.

One of the predictions of this model is that short-lived sunspots serve as triggers for flares. The short-lived population of sunspots is most probably associated with emergence of new magnetic flux (Rust and Bridges, 1975). The possible association between the birth of short-lived satellite groups and the generation of flares was reported by Krivsky (1977). The satellite sunspot groups is the local trigger of flares that does not exclude a more global trigger. The global trigger was possibly seen in sympathetic flare phenomena in several active region as simultaneously observed by Ogir (1981). In general, the centripetal character of the longitudinal ( $R_\varphi$ ) anisotropy of the flares together with the “sheared” behaviour of the latitudinal ( $R_\lambda$ ) anisotropy at the  $\varphi - t$ -diagram may be well understood in terms of the global triggering scenario of flares as suggested in this paper.

### References

- Allen, C. W. (1955) *Astrophysical Quantities*, Lon., Athlon Press, 304p.  
Antalova, A., Gnevyshev, M. N. (1983) *Contr. Astron. Observ. Skalnaté Pleso* 11, 63.  
Blazhko, C. H. (1954) *Course Spherical Astronomy*, GITL, Moscow, 180p. (in Russian).  
Gershberg, R. E., Mogilevsky, E. I., Obridko, V. N. (1987) *Kinematics and Physics of Space Bodies* 3, No. 5, 3 (in Russian).

- Gibson, E. G. (1973) *The Quiet Sun*, NASA, Wash. D.C., 330p.
- Krivsky, L. (1977) *Solar Proton Flares and Their Prediction*, Prague, Acad., 121p.
- Krivsky, L., Knoska, S. (1967) *Bull. Astron. Inst. Czech.* **18**, No. 6, 325.
- Kasinsky, V. V. (1973) *Solar Data Bulletin*, No.7, 77.
- Kasinsky, V. V., Krat, V. A. (1973) *Solar Physics* **213**, 219.
- Kasinsky, V. V. (1981) *Physica Solariterr. Potsdam.* **17**, 37.
- Kasinsky, V. V. (1988) *Issled. po Geomagnetizmu Aeronomii i Fizike Solntsa*, Nauka, Moscow **79**, 25.
- Kasinsky, V. V. (1989) In: R. A. Gulyaev (ed.), *Atmosphere of the Sun, Interplanetary Space, and Planetary Atmospheres*, IZMIRAN Press, Moscow, 116 (in Russian).
- Kasinsky, V. V. (1994) *Issled. po Geomagnetizmu Aeronomii i Fizike Solntsa*, Nauka, Novosibirsk **102**, 152.
- Mogilevsky, E. I. (1980) *Physics of Solar Activity*, Nauka, Moscow, 3 (in Russian).
- More, D. W. (1964) *Astrophys. Journ.* **131**, No. 1, 78.
- Ogir, M. B. (1981) *Izvestiya Krymskoi Astrofiz. Obs.* **64**, 118.
- Pogodin, I. E. (1977) *Dokl. AN SSSR* **234**, No. 6, 1284.
- Rust, D. M., Bridge, C. A. (1975) *Solar Physics* **43**, 129.
- Somov, B. V. (1981) *Solar Maximum Year*, Nauka, Moscow **1**, 155 (in Russian).
- Syrovatsky, S. I. (1966) *Astron. J.* **43**, 340.
- Quarterly Bulletin of Solar Activity* (1935–1976) IAU, Zurich.